Publishing House
AKAPIT

COMPUTER METHODS IN MATERIALS SCIENCE

Informatyka w Technologii Materiałów

Vol. 10, 2010, No. 2

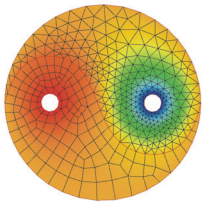

PHYSICAL AND NUMERICAL MODELLING OF PLASTIC DEFORMATION OF MAGNESIUM ALLOYS

DARIUSZ KUC[1], MACIEJ PIETRZYK[2]

[1]Politechnika Śląska, ul. Krasińskiego 8, 40-019 Katowice
[2]Akademia Górniczo-Hutnicza, al. Mickiewicza 30, 30-059 Kraków
**Corresponding Author: e-mail Dariusz.Kuc@polsl.pl*

Abstract

Proposition of a new material model accounting for twinning and slip is described in the paper. The model was developed on the basis of physical and numerical simulations of hot deformation of magnesium alloy. Slip is base deformation mechanism in a majority of alloys but twinning occurs for example in some special steels or in the investigated in the present work magnesium alloys. The model is based on the internal variable method. This method is well researched for slip. In the proposed model twinning is treated as pseudo-slip with the twins volume fraction being a dependent variable. Experimental tests for the AZ31 alloy were performed and inverse analysis was applied for identification of the models parameters. The results obtained for the closed form equations and for the internal variable model are compared in the paper. It is shown that the latter model accounts for accommodation of strains by twinning and better reproduces behaviour of the alloy at the beginning of deformation.

Key words: modelling flow stress, twinning, magnesium alloys, internal variable

1. INTRODUCTION

For years rheological models used for simulation of processing of materials have been based on static function of such external variables as temperature, strain rate and strain (Grosman, 1997; Schindler & Hadasik, 2000; Pietrzyk et al., 2006). It is, however, observed in experiments that microstructural changes in metals and alloys, caused by changes of the external variables, require some time, and delay in response may be observed (Urcola & Sellars, 1987). Thus, a kinetics of the process has to be considered. New material models, which use time as independent variable, were developed to account for this phenomenon (Davies, 1994). Internal variables are the dependent variables in these models, which are successfully used to predict behaviour of materials during deformation when slip is a dominant mechanism. There are, however, several alloys which involve two deformation modes possible in polycrystalline materials: slip and twinning. Magnesium alloys are an example of such materials. Less research has been performed on the modelling of the twining mechanism. Among the solutions available in the literature those based on the Taylor model (Barnett, 2003) and on the semianalytical Sachs model (Barnett et al., 2006) should be mentioned. An alternative proposition based on the internal variable approach is the objective of the present work. The physical and numerical simulations of deformation of magnesium alloy were performed and the results were used to develop the flow stress model for polycrystals, in which mechanism of twinning contributes to deformation. The developed model is general for all the polycrystals deformed by

 ISSN 1641-8581

twinning, but identification of the model was performed for the selected AZ31 magnesium alloy.

2. PHYSICAL SIMULATION

Bars of ϕ 15mm after hot rolling, made from alloy AZ31 (ASTM designation) constituted the experimental material. The chemical composition (in wt%) of AZ31 was: 2.83 %Al, 0.8%Zn, 0.37%Mn and 0.002%Cu. The microstructure of alloy specimens in initial state, after annealing is shown in figure 1. The alloy is characterized by a single-phase microstructure.

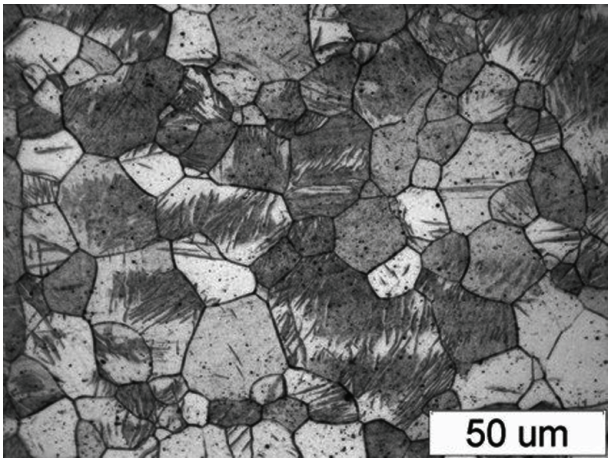

Fig. 1. *Microstructure of invesigated alloy after hot rolling and annealing at 450°C.*

The uniaxial compression tests were performed on the Gleeble 3800 thermomechanical simulator at the Institute for Ferrous Metallurgy in Gliwice, Poland. The AZ31 samples measuring ϕ10×12 mm were deformed at temperatures 200 - 450°C and at strain rates 0.01 – 10 s^{-1}. These conditions were selected to cover the expected range of temperatures and strain rates observed during forming of the AZ31 alloy. The total strain measured as the height reduction ($\varepsilon = \ln(h_1/h_2)$, where h_1, h_2 – height of the sample before and after the test) was $\varepsilon = 1$. Load vs. displacement data were monitored at each test. Beyond this, surface temperature of the sample was measured. Selected example of the registered loads and temperatures is shown in figure 2.

Analysis of the measurements shows that the temperatures of the sample varies during the test at higher strain rates. Since the heat capacity of the magnesium alloy is reasonably low, more than two times lower then for steel, the effect of the deformation heating is important for this material. However, the variations of the temperature are due not only to the deformation heating, but also to the temperature control system on the Gleeble 3800 simulator, see for example the curve for the strain rate of 1 s^{-1} in figure 1b. All these facts are accounted for in the inverse analysis of the tests.

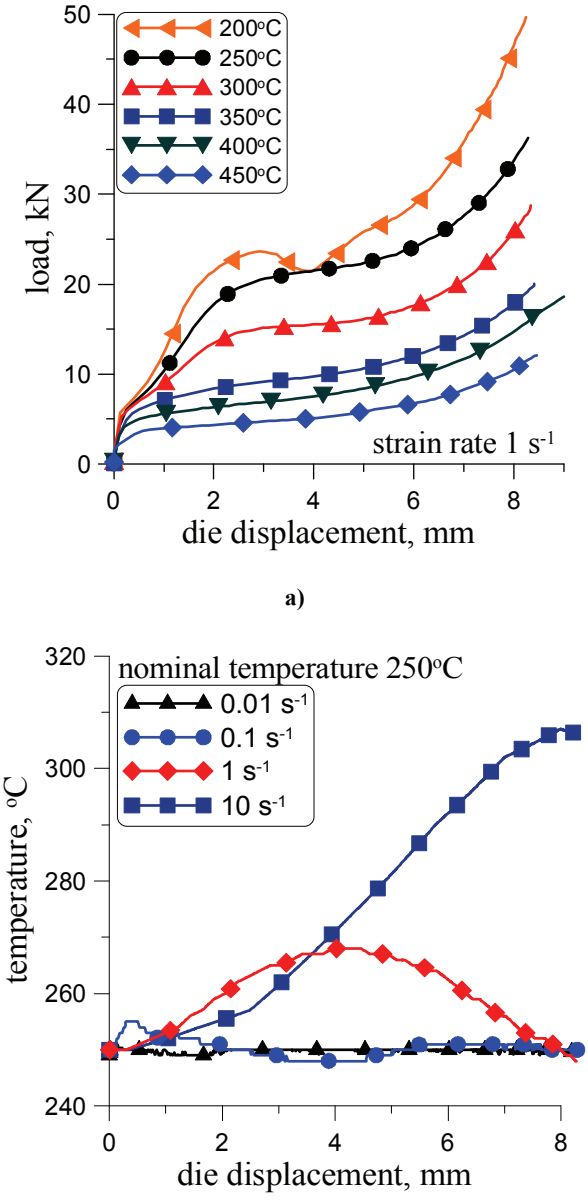

Fig. 2. *Recorded load vs. die displacement data at the strain rate of 1 s^{-1} (a) and temperatures during the tests performed at the nominal temperature of 250°C (b).*

3. MECHANISMS OF DEFORMATION OF THE AZ31 ALLOY

There are two main mechanisms of deformation of polycrystalline materials: slip and twinning. Twinning is a mechanism occurring for example in magnesium alloys or in some special steels (TWIP – twinning induced plasticity). Majority of magnesium alloys crystallize with hexagonal close packed (hcp) structure and they have very limited number of slip

systems at room temperature, which results in a poor ductility. Besides slip, twinning is another intragranular plastic deformation mode and there are many twinning systems in magnesium alloys. Typical flow curves, which illustrate the influence of temperature on the flow stress changes as a function of the deformation of the AZ31 magnesium alloy during the hot compression, are presented in figure 3a. These results indicate that a decrease in the test temperature from 350 to 300°C causes a radical changes in character of flow curve, what coincides with the observations of Beer and Barnett (2006). It is confirmed by figure 3b, where instantaneous work hardening coefficient vs. strain is shown. Decrease and increase of this coefficient with increasing strain is observed at 250 and 300°C, while monotonous decrease of the coefficient is obtained at higher temperatures.

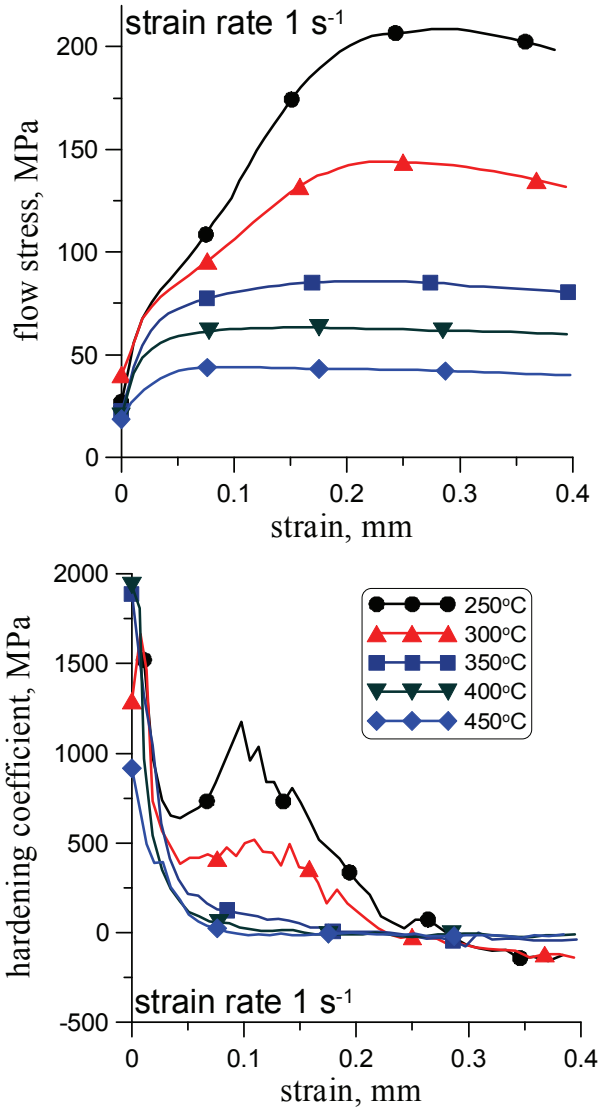

Fig. 3. Stress-strain curves (left) and hardening coefficient (right) of AZ31 alloy obtained during deformation at temperatures from 250℃ to 450℃ and strain rate 1s^{-1}. (Meaning of the symbols is the same in both plots).

The influence of the hot deformation on the microstructure of the AZ31 alloy is shown in figure 4. The structure of the alloy after deformation at a temperature of 250 and 300°C with deformation rate 0.1 s^{-1} consists of elongated primary grains with their boundaries deformed and many deformation twins (figure 4a). A rise in the test temperature to 350°C reduces number of twins (figure 4b).

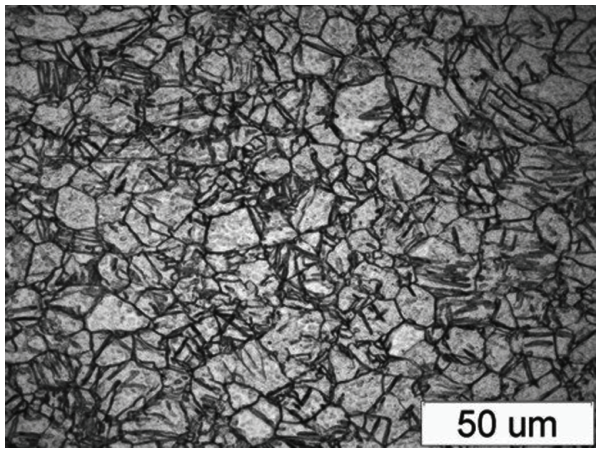

a)

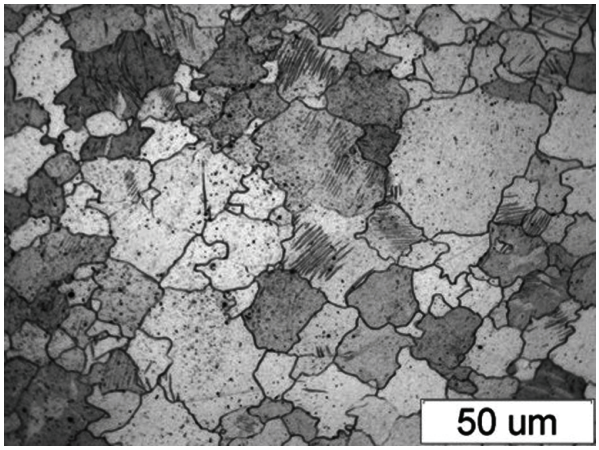

b)

Fig. 4. Structure of hot deformed AZ31 alloy after deformation at a strain rate 1s^{-1} and temperature 250℃ (a) and 350℃ (b) to deformation $\varepsilon = 0.1$.

4. INTERNAL VARIABLE MODEL (IVM)

The slip is reasonably well researched and accounted for in modelling based on the internal variable method. Less research has been performed on twinning. Both mechanisms are considered below and an attempt to build the general IVM model is made.

4.1. Slip

Resistance to deformation in slip is an effect of competing mechanisms of hardening (increase of

flow stress) and dynamic softening (decrease of flow stress due to recovery or recrystallization). In mathematical models, which account for these mechanisms, the density of defects in the material is used as a dependent variable, which is a function of time and of external variables describing conditions of the process, eg. temperature. Dislocations are the only defects, which are usually considered. Such model is based on fundamental works of Mecking and Kocks (1981), and Estrin and Mecking (1984), which are summarized by Estrin (1996). The numerical model used in the present work is described by Ordon et al. (2000).

Since the stress during plastic deformation is governed by the evolution of dislocation populations, a competition of storage and annihilation of dislocations, which superimpose in an additive manner, controls a hardening. The flow stress is proportional to the square root of dislocation density:

$$\sigma = \sigma_0 + \alpha b \mu \sqrt{\rho} \tag{1}$$

where: ρ – dislocation density [m^{-2}], σ_0 – stress accounting for elastic deformation [MPa], α – coefficient, b – length of the Burgers vector [m], μ – shear modulus [MPa].

The evolution of dislocation populations accounting for hardening and recovery is:

$$\frac{d\rho(t)}{dt} = \frac{\dot{\varepsilon}}{bl} - M\rho(t) \tag{2}$$

where: $\dot{\varepsilon}$ – strain rate [s^{-1}], l – free path for dislocations [m], M – the mobility of recovery [s^{-1}].

Since analysis of the primary stage of deformation is the objective of the paper, the effect of dynamic recrystallization is neglected in this approach. Assuming that strain rate $\dot{\varepsilon}$ and dislocation density ρ are an input and output variables, respectively, we obtain:

$$B\frac{d\rho}{dt} + \rho = k\dot{\varepsilon} \tag{3}$$

where: $B = 1/M$ – time constant [s], $k = 1/(blM)$ – coefficient [s/m^2].

Since internal variable model is time dependent, further analysis in this work will be based on the control theory. Applicability of this theory to modelling of materials processing, accounting for the microstructure evolution, is confirmed in Svetlichnyy (2004). Equation (3) is the same as for the first order inert object in the control theory. Electrical two-pair terminal network representing such an object is shown in figure 5a, where: R – resistance, C – capacity. Laplace transmittance of this element is:

$$G(s) = \frac{k}{Bs+1} \tag{4}$$

where: s – Laplace operator

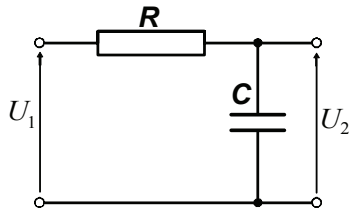

a)

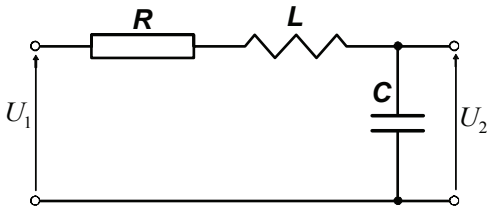

b)

Fig. 5. *Two-pair terminal network a - RC and b - RLC.*

Relation between electrical and material constants is: $B = RC = 1/M$. Amplifying coefficient $k = 1$ for the electrical circuit and $k = 1/(blM)$ for the material model.

This approach is well known. When temperature is constant or temperature dependence of coefficients is neglected, equation (3) is linear and solution is simple, for example material response to the input step function:

$$\dot{\varepsilon}(t) = \begin{cases} 0 & \text{for } t < 0 \\ \dot{\varepsilon}_0 & \text{for } t \geq 0 \end{cases} \tag{5}$$

is:

$$\rho(t) = k\dot{\varepsilon}_0 \left[1 - \exp\left(\frac{-t}{B} \right) \right] \tag{6}$$

In real industrial processes temperature changes and nonlinear equation (3) has to be solved numerically, see (Davies, 1994; Ordon et al., 2000). Figure 6 shows response of the system for the compression tests, in which input variable (strain rate) changes by a step function

$$\dot{\varepsilon}(t) = \begin{cases} \dot{\varepsilon}_1 & \text{for } \varepsilon < 0.25 \\ \dot{\varepsilon}_2 & \text{for } \varepsilon \geq 0.25 \end{cases} \tag{7}$$

at the strain of 0.25. Results for both increase (ε_1 = 1 s^{-1}, ε_2 = 10 s^{-1}) and decrease (ε_1 = 10 s^{-1}, ε_2 = 1 s^{-1}) of the strain rate are shown and compared with the experimental data (Ordon et al., 2000). These results were obtained for an austenitic steel. Flow stress is calculated using equation (1). It is seen that delay of the response is particularly important when the strain rate increases rapidly.

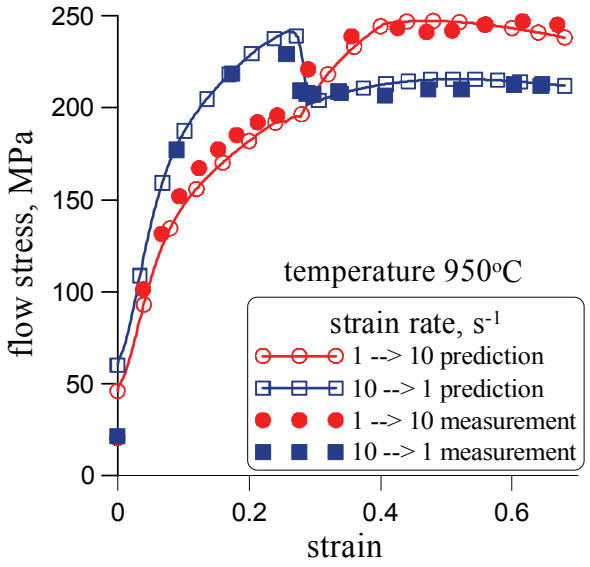

Fig. 6. *Stress-strain curve measured and predicted by the IVM model in the varying strain rate test for an austenitic steel.*

4.2. Twinning

Twinning is based on the homogenous displacement of crystal layers in the parallel planes to the twinning plane and it does not involve increase of the dislocation density. In some of published works twinning is, however, modelled as pseudo-slip, see for example (Prakash et al., 2008). In this model the twin volume fraction f is a dependent variable which, similarly to the dislocation density in slip, is a function of time and of external variables. Evolution of the twin fraction is:

$$\frac{df}{dt} = \frac{\dot{\varepsilon}}{S} \quad \text{for} \quad \tau > 0 \qquad \frac{df}{dt} = 0 \quad \text{for} \quad \tau \le 0 \qquad (8)$$

where: τ – shear stress [MPa], S – characteristic shear of the twin (0.707 for cubic materials).

4.3. Combined effect of twinning and slip

Usually both mechanisms, twinning and slip, contribute to deformation of metals such as magnesium alloys or in some special steels e.g. TWIP steels (twinning induced plasticity). Their effect is different at different stages of deformation and at various conditions (temperatures, strain rates). It is seen in figure 7, where comparison of the flow stress for a C-Mn steel and magnesium alloy AZ31 is shown. Plots up to the strain of 0.3 only are shown.

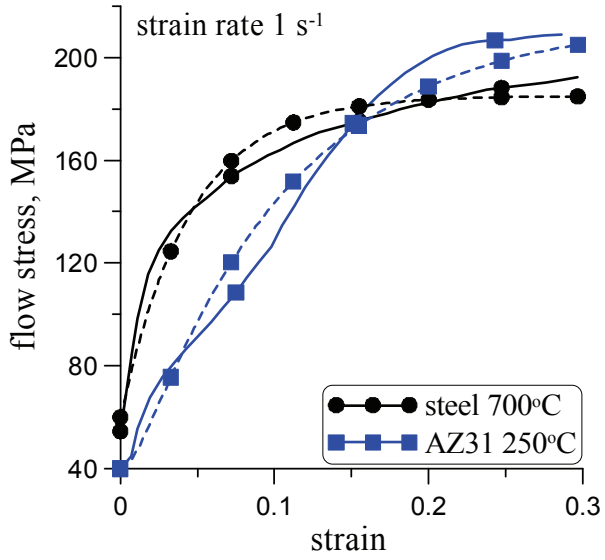

Fig. 7. *Experimental (solid lines) and predicted (dotted lines) flow stress of C-Mn steel (no twinning) and AZ31 alloy (with twinning) as a response to the constant strain rate deformation.*

This plot can be treated as the response of the material to the input step function (4) with $\dot{\varepsilon}_0$ = 1 s^{-1}. Since two different materials deformed at different temperatures are presented, figure 7 can be considered as demonstration only and the two curves should be compared qualitatively. Effect of twinning in steels is negligible and character of the response shows that this material is described well by equation (3) - the first order inert object. Contrary, the mechanism of twinning is important in AZ31 for lower strains while slip occurs at larger strains.

The next objective of the present work is applying the concept of the internal variable method to modelling metallic materials, in which both twinning and slip contribute to the deformation, as discussed in chapter 2. The approach is based on the presented by Madej and Pietrzyk (2009) concept of equivalence between material exposing two deformation mechanisms and the electrical circuit composed of the resistance, inductance and capacity. It is assumed that twinning accommodates some part of the strain rate what, in consequence, leads to slower than expected increase of the dislocation density. The role of twinning in plastic deformation of materials is similar to the role of an inductance in the electrical circuit shown in figure 5b. Assuming that change of dislocation density caused by twinning is propor-

tional to the volume fraction of twins ($f = c\partial\rho/\partial t$), the second order inert term is obtained:

$$B_2^2 \frac{d^2\rho}{dt^2} + B_1 \frac{d\rho}{dt} + \rho = k\dot{\varepsilon} \tag{9}$$

Time constants in this equation are:

$$B_1 = \frac{1}{M} \qquad B_2 = \sqrt{\frac{Sc}{blM}} \tag{10}$$

When temperature is constant or temperature dependence of coefficients is neglected, equation (9) is linear and solution is simple, for example material response to the input step function (5) is:

$$\rho(t) = \dot{\varepsilon}_0 k \left\{ 1 - \frac{1}{B_1 - B_2} \left[B_1 \exp\left(\frac{-t}{B_1}\right) - B_2 \exp\left(\frac{-t}{B_2}\right) \right] \right\} \tag{11}$$

Results of simulation of deformation using equations (4), (5), (6), (8) and (9) are shown by dotted lines in figure 5. Reasonably good agreement with the experiment is observed. This is the first approach to this model and further research described in chapter 5 should improve accuracy of the solution.

4.4. Testing of the model

Numerical tests were performed to show capabilities of the model. Figure 8 shows comparison of the response of the model for various relative values of time constants B_1 and B_2. The results are recalculated to the stress-strain relation following equation (1). It is seen from this figure that the model is capable to predict delay of the response due to twinning. This delay is larger when constants S and c are larger.

5. IDENTIFICATION OF THE MODEL

Analysis of results of axisymmetrical compression of AZ31 is the objective of this part of the work. The plastometric tests were performed to determine the flow stress model for this alloy, which is needed for numerical simulations of forming processes (Rauch et al., 2008). Inverse analysis was applied to eliminate the influence of various disturbances on the results of the plastometric tests and to determine the flow stress of this material independent of the inhomogeneities in the tests.

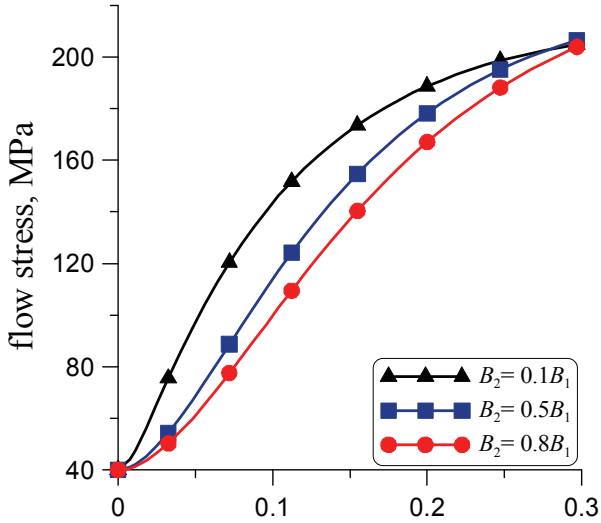

Fig. 8. Comparison of the response of the model for various relative values of time constants B_1 and B_2 in equation (8).

5.1. Inverse algorithm

Due to various disturbances (effect of friction, deformation heating etc), different plastometric tests involve different strain distribution and inhomogeneities of deformation. Thus, direct comparison of results of various tests is difficult. It is shown in a number of publications (Gavrus et al., 1996; Szyndler et al., 2001; Forestier et al., 2002) that application of the inverse analysis to the interpretation of plastometric tests minimizes the influence of these disturbances and allows flow stress to be determined independent of the method of testing. The inverse method is applied in the present work to interpret the results of the axisymmetrical compression tests performed for the AZ31 alloy samples.

Friction factor has to be known to determine the flow stress, therefore, this factor determined for the Gleeble simulator in (Szyndler et al., 2001) and equal 0.12 was used in the present project. Inverse algorithm described in (Szeliga et al., 2006) is used in the present analysis. The flow stress model is identified by searching for the minimum of the objective function, which is defined as a square root error between measured and calculated loads:

$$\Phi = \sqrt{\frac{1}{Npt}\sum_{i=1}^{Npt}\left[\frac{1}{Nps}\sum_{j=1}^{Nps}\left(\frac{F_{cji}(\mathbf{x},\mathbf{p}_i) - F_{mji}}{F_{mji}}\right)^2\right]} \tag{12}$$

where: F_{mij}, F_{cij} – measured and calculated loads, Npt – number of tests, Nps – number of load measurements in one test, $\mathbf{p}$ – vector of process parameters (strain rates, temperatures), $\mathbf{x}$ – vector of coeffi-

cients in the models (rheological parameters, friction coefficient).

The direct problem model, which in the inverse analysis simulates the experiment, is based on the finite element program described by Pietrzyk (2000) and is defined as simulation of the axisymmetrical compression tests. The finite element code used in the calculations is based on the rigid-plastic approach coupled with the solution of the heat transport equation. Detailed description of this model is given in Lenard et al.'s work (1999) and the main equations and assumptions are presented briefly below. The approach follows the extremum principle, which states that for a plastically deforming body of volume Ω, under the tractions $\underline{\boldsymbol{\tau}}$ prescribed on the part of the surface Γ_t and the velocity $\mathbf{v}$ prescribed on the remainder of the surface Γ_v under the constraint $\dot{\varepsilon}_V = 0$, the actual solution minimizes the functional:

$$J = \int_{\Omega} \left(\sigma_i \dot{\varepsilon}_i + \lambda \dot{\varepsilon}_V \right) d\Omega - \int_{\Gamma_t} \underline{\boldsymbol{\tau}}^T \underline{\mathbf{v}} d\Gamma_t \qquad (13)$$

where: λ – Lagrange multiplier, σ_i – effective stress which, according to the Huber-Mises yield criterion, is equal to the flow stress σ_p, $\dot{\varepsilon}_i$ - effective strain rate, $\dot{\varepsilon}_V$ – volumetric strain rate, $\underline{\boldsymbol{\tau}} = \{\tau_r, \tau_z\}^T$ – vector of boundary traction, $\underline{\mathbf{v}} = \{v_r, v_z\}^T$ – vector of velocities, v_x, v_y – components of the velocity vector, τ_r, τ_z – components of external stress, which in plastometric tests is a friction stress.

In the flow theory of plasticity, strain rates ($\underline{\dot{\boldsymbol{\varepsilon}}}$) are related to stresses ($\underline{\boldsymbol{\sigma}}$) by the Levy-Mises flow rule:

$$\underline{\boldsymbol{\sigma}} = \frac{\sigma_p}{3\dot{\varepsilon}_i} \underline{\dot{\boldsymbol{\varepsilon}}} \qquad (14)$$

Discretization of equation (13) and differentiation with respect to the nodal velocities and to the Lagrange multiplier yields a set of non-linear equations, which is usually solved by the Newton-Raphson linearization method. Linearization yields:

$$\mathbf{p} = \mathbf{K} \begin{Bmatrix} \Delta \mathbf{v} \\ \lambda \end{Bmatrix} \qquad (15)$$

where:

$$\mathbf{K} = \begin{bmatrix} \dfrac{\partial^2 J}{\partial \mathbf{v}^T \partial \mathbf{v}} & \mathbf{b} \\ \mathbf{b}^T & 0 \end{bmatrix} \quad \mathbf{p} = \begin{Bmatrix} \dfrac{\partial J}{\partial \mathbf{v}^T} \\ \mathbf{b}^T \hat{\mathbf{v}} \end{Bmatrix} \quad \mathbf{b} = \int_V \mathbf{B}^T \mathbf{c} dV \qquad (16)$$

where: $\hat{\mathbf{v}}$ – vector of nodal velocities calculated in the previous iteration, $\Delta \mathbf{v}$ – vector of increments of nodal velocities, $\mathbf{c}$ – matrix, which imposes the incompressibility condition $\dot{\varepsilon}_V = \mathbf{c}^T \underline{\dot{\boldsymbol{\varepsilon}}}$ – volumetric strain rate, $\mathbf{B}$ – matrix of derivatives of shape functions.

The friction model proposed by Chen and Kobayashi (1978) and described also in (Lenard et al., 1999) is used in this approach:

$$\tau = m \frac{\sigma_p}{\sqrt{3}} \left[\frac{2}{\pi} \tan^{-1} \left(\frac{|\mathbf{v}_s|}{a} \right) \right] \qquad (17)$$

where: m – friction factor, $\mathbf{v}_s$ – slip velocity, a – constant, few orders smaller than an average slip velocity (if the value of slip velocity $\mathbf{v}_s$ is large, formula (17) is equivalent to Tresca friction law $\tau = mk$ with k – yield stress in shear.

It was observed in the experiments that deformation heating causes an increase of the sample temperature in the plastometric tests. Proper prediction of the temperature increase is an inevitable condition for obtaining realistic results. Therefore, the flow formulation, which is the basis of the mechanical model in the present work, is coupled with the finite element solution of the Fourier heat transfer equation:

$$\nabla \cdot k \nabla T + Q = c\rho \frac{\partial T}{\partial t} \qquad (18)$$

where: k – conductivity, Q – heat generation rate due to deformation work, c – specific heat, ρ – density, T – temperature, t – time.

The following boundary conditions are used in the solution:

$$k \frac{\partial T}{\partial \mathbf{n}} = q + h\left(T_a - T\right) \qquad (19)$$

where: h – heat transfer coefficient, T_a – surrounding temperature or tool temperature, q – heat flux due to friction, $\mathbf{n}$ – unit vector normal to the surface.

The following thermophysical parameters were assumed in the paper: density ρ = 1738 kg/m^3, conductivity k = 156 W/(mK) and specific heat c = 1020 J/(kgK). Discretization of the problem is performed in a typical finite element manner (Zienkiewicz & Taylor, 1989) using quadrilateral 4 node elements for mechanical part and 12 node elements for thermal part. Simulations of plastometric tests were performed using this software.

5.2. Results for conventional models

The inverse analysis of rheological law was performed in 2 steps, as shown in Szeliga et al.'s work (2006). The flow stress as a function of strain given in a tabular form for each test separately was determined first and the results are presented in figure 9. This flow stress, when implemented into the finite element code, gives perfect agreement between the measured and predicted loads during the tests.

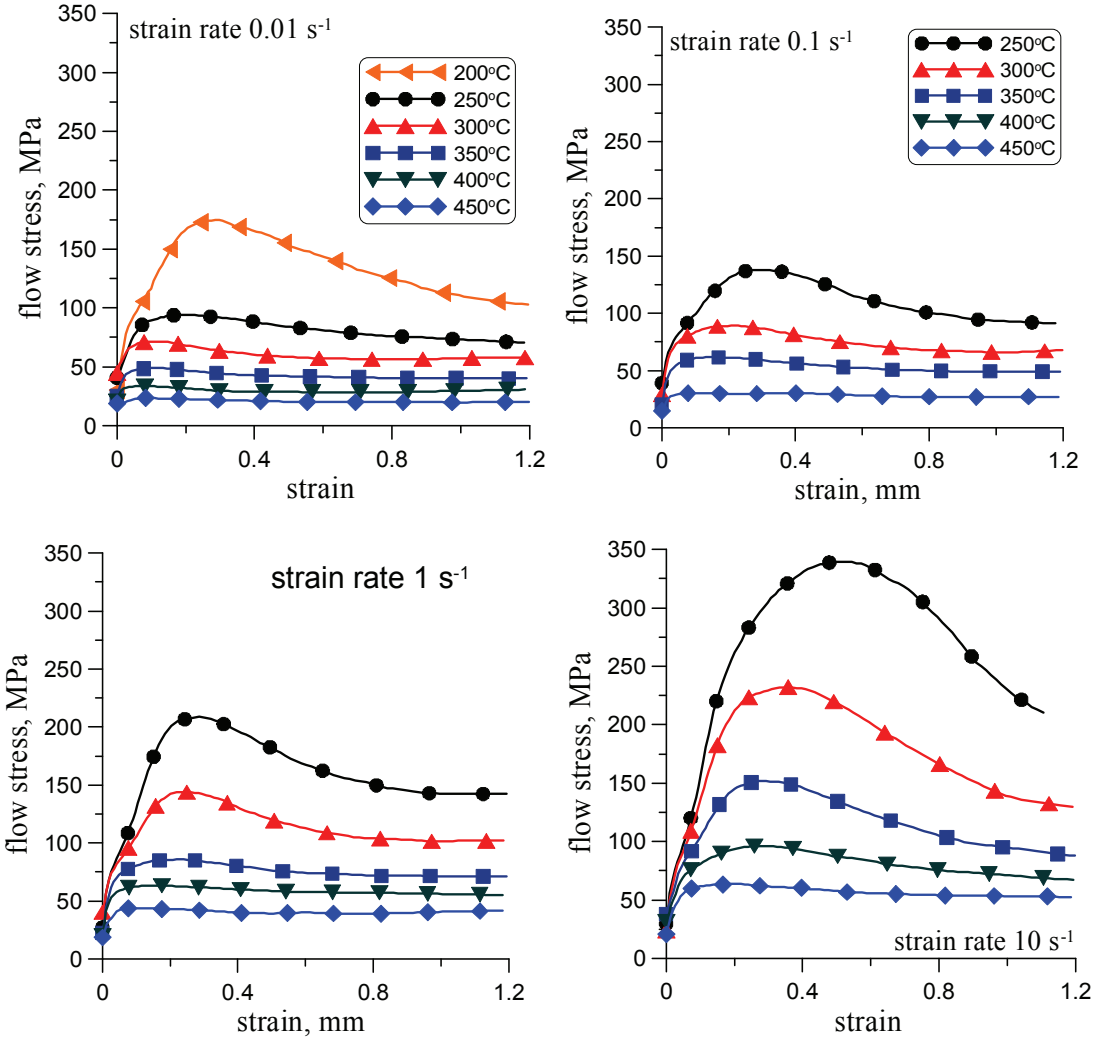

Fig. 9. *Flow stress determined in the first step of the inverse analysis as function of strain for the AZ31 alloy (meaning of the symbols is the same in all plots).*

Identification of coefficients in the flow stress model was the objective of the second part of the inverse analysis. These coefficients were the variables in the objective function (12), which is defined as a square root error between measured and predicted loads in all tests performed for the investigated steels. It is expected that when the flow stress function is introduced in the FE code, the agreement between measured and predicted loads may not be as perfect as in the case of the stress-strain relation introduced in a tabular form. The agreement in this case depends on the function's capability of reproducing properly behaviour of the deformed material, which is not always easy. Several functions were tested within the project and the two of them were selected. The first is Hansel and Spittel (1978) equation:

$$\sigma_p = A\varepsilon^n \exp\left(-B\varepsilon\right)\dot{\varepsilon}^m \exp\left(-CT\right) \qquad (20)$$

The second considered model is a modification of the equation proposed in (Gavrus et al., 1996):

$$\sigma_p = \sqrt{3}\left[a\varepsilon^n \exp\left(\frac{\beta}{T+273}\right)\exp\left(-q\varepsilon\right)+ \left[1-\exp\left(-q\varepsilon\right)\right]a_{sat}\exp\left(\frac{\beta_{sat}}{T+273}\right)\right]\left(\sqrt{3}\dot{\varepsilon}\right)^m \qquad (21)$$

where: ε – strain, $\dot{\varepsilon}$ – strain rate, T – temperature, °C,

Table 1. *Coefficients in equations (20) and (21) obtained from the inverse analysis for the AZ31 alloy.*

Eq.	A	n	B	m	C			Φ
(20)	2517	0.339	0.978	0.148	7.459			0.1146
Eq.	a	β	n	m	a_{sat}	β_{sat}	q	Φ
(21)	0. 12047	2683.3	0. 351	0. 1578	0.2675	2754.9	1.645	0.1166

Table 2. *Coefficients in the Sellars and McTegart (1966) equation obtained from the inverse analysis for the AZ31 alloy – notation of coefficients is the same as in (Hadasik et al., 2006).*

A_0	n_0	α_0	A_{sse}	n_{sse}	α_{sse}	A_{ss}	n_{ss}	Φ
$0.717 \cdot 10^{11}$	18.19	0.025	$0.912 \cdot 10^{13}$	2.59	0.02	$0.286 \cdot 10^{12}$	4.15	
α_{ss}	q_1	Q_2	C_c	N_c	C_x	N_x	Q_{def}	0.137
0.0336	0.8	0	0.00168	0.038	0.0045	0.198	175160	

dynamic recrystallization. Therefore, the equation proposed originally by Sellars and McTegart (1966) containing 16 coefficients was also considered. This is a complex equation, which is published in a number of publications (see for example Kowalski et al., 2000; Hadasik et al., 2006), and is not repeated here.

The values of the coefficients in the investigated equations, determined using inverse analysis are given in

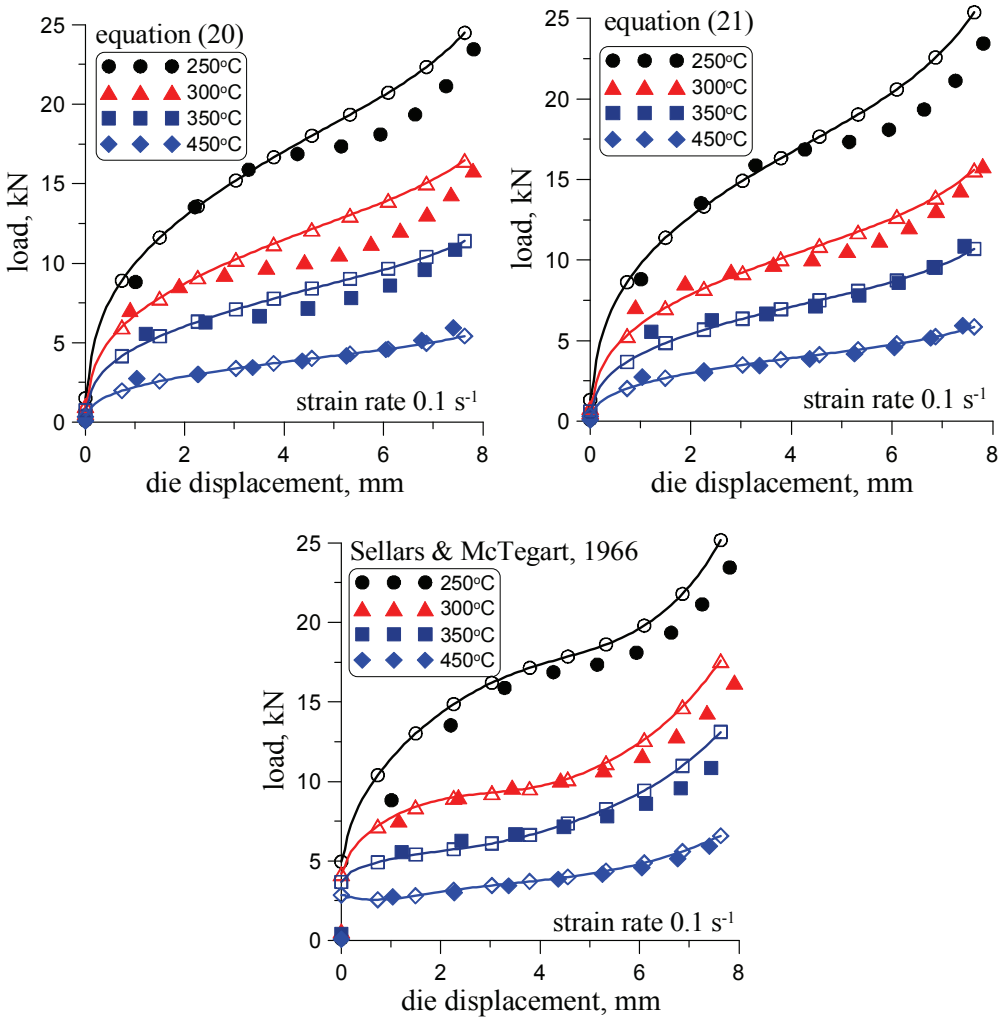

Fig. 10. *Comparison of measured loads (filled symbols) with results of FE calculations using various models with coefficients in tables 1 and 2 as rheological law (open symbols), for the AZ31 alloy. Shape of the symbol distinguishes the temperature of the test.*

There are 5 coefficients in equation (20) and 7 coefficients in equation (21). These models are not flexible enough to reproduce properly stress strain curves composed of hardening, peak stress, softening and saturation, which are characteristic for the table 1. Values of the objective function (12), which represent an accuracy of the inverse analysis, are also given in this table. It is concluded that accuracy of the solution is low for all considered functions.

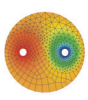

Figure 10 shows an example of comparison of the loads measured in the tests and calculated by the FE program with the investigated equations implemented in the constitutive law. These plots confirm that the equations are not capable to reproduce the behaviour of the AZ31 alloy in the whole range of the considered temperatures and strain rate. Very good agreement between measurements and predictions of loads was obtained for the higher temperatures. Accuracy is not so good in lower temperatures, when twining mechanism becomes more important. The models calculated base on Hansel and Spittel (1978) equation (21), Gavrus et al.'s (1996) equation (22) and Sellars and McTegart (1966) equation were developed mainly for steels where the slip is dominated mechanism of deformation. It can be seen in figure 9 that with decreasing temperature and increasing of strain rate, the shape of the flow curve changes, and this can be attributed to the onset of twinning. The intensive twinning has influence on higher level of stress, at lower deformation temperature. In spite of this facts presenting equation gives worse compatibility in lower temperature with the experimental results.

6. IDENTIFICATION OF THE INTERNAL VARIABLE MODEL

6.1. Numerical solution

Solution of equation (9) for nonlinear coefficients can be performed using numerical methods. Finite difference method is one of the possibilities. In the present paper, however, simplified approach was considered first to evaluate the capabilities of the model to reproduce qualitatively behaviour of the materials deformed by two mechanisms. The flow stress was calculated from equation (11) with the coefficients dependent on temperature and strain rate. The following relationships were used 22-25:
Average free path for dislocations

$$l = \frac{a_1}{Z^{a_4}} \tag{22}$$

Mobility coefficient for recovery process

$$m = a_2 \dot{\varepsilon}^{a_7} \exp\left(\frac{-a_3}{R\widehat{T}}\right) \tag{23}$$

Coefficient, which controls effect of twinning on dislocation density

$$c = 10^{-17} a_5 \left[1 + \left(\frac{a_9}{t}\right)^3\right] \tag{24}$$

Shear modulus

$$\mu = 176400 + 192T \tag{25}$$

where: $\widehat{T}$ – temperature in K, T – temperature in °C, t – time $\dot{\varepsilon}$ – strain rate, Z – Zener-Hollomon parameter calculated for the activation energy a_8, R – gas constant. Beyond this the length of the Burgers vector for the AZ31 alloy is assumed as 0.321×10^{-9}, coefficient α in equation (1) was considered as optimization variable $\alpha = a_6$. The stress σ_0 in equation (1) is a function of temperature, which on the basis of experiments is assumed as: $\sigma_0 = 51.35\text{-}0.071T$.

There are 9 coefficients in the model, which are determined using inverse software described in section 4.1. Since the influence of twinning is negligible at higher strains, the identification was performed for the strains to 0.3. The values of coefficients $\mathbf{a} = \{a_1, \ldots a_1\}$ obtained from the inverse calculations and the final value of the objective function are given in table 3. Since flow stress is not measured directly in the test, validation of the model by comparison of measured and predicted stresses is not possible. The primary validation was performed assuming that the flow stress determined in the first step of the inverse analysis can be considered as the measured flow stress. Comparison was made only for one test and for the beginning of deformation, in which the influence of twinning is important. The result is presented in figure 10. It is seen in this figure that the model based on the second order inert term has the capability to reproduce properly the shape of the flow stress curve.

The full validation was performed by comparison loads, which are directly measured on the Gleeble 3800 system. The results of this validation of the model are shown in figure 10. Comparison of the loads measured in the tests and predicted by the FE code with the IVM model with coefficients in table 3 as the rheological law, confirmed good accuracy of the model.

Table 3. *Coefficients in internal variable model obtained from the inverse analysis for the AZ31 alloy.*

a_1	a_2	a_3	A_4	a_5	a_6	a_7	a_8	a_1	Φ
0.0137	6343	32502	0.5368	0.0129	1	1.0765	50635	280	0.1166

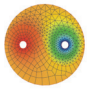

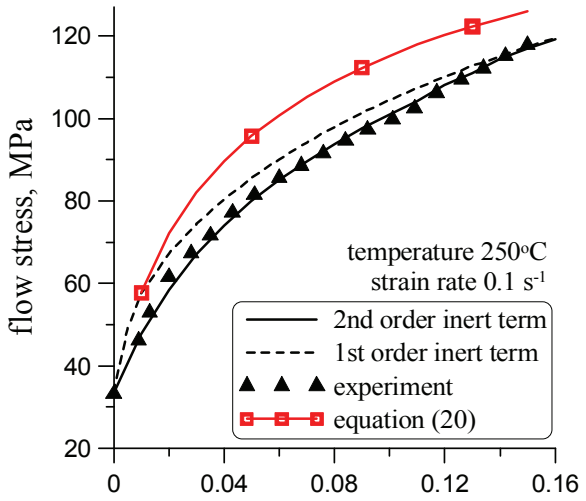

Fig. 11. Comparison of the flow stress obtained from the first step of the inverse analysis with that calculated from the two considered models, for the AZ31 alloy.

Analysis of results shows that the IVM model allows much better description of the AZ31 alloy behaviour than conventional closed form equation. The final value of the objective function decreased from about 11-13% for the closed form equations to below 8% for the IVM model. This improvement is due mainly to the capability of the IVM model to reproduce slowing down of hardening at the beginning of deformation due to twinning mechanism. In consequence better reproduction of loads for small strains is obtained.

7. CONCLUSIONS

A proposition of a new material model, accounting for both twinning and slip, is described in the paper. The model is based on the internal variable method (IVM). This method is well researched for slip. In the proposed model twinning is treated as pseudo-slip with the twin volume fraction f being a dependent variable. Presented analysis and results allow to draw the following conclusions regarding applicability of the models:

– Contribution of twinning is that it accommodates part of the strain rate and causes slower evolution of the dislocation density at the beginning of deformation.
– Mathematical description of the accommodation of the strain rate due to twinning can be based on the control theory. In consequence, the evolution of the dislocation density accounting for both twinning and slip can be described by the equations developed for the second order inert term.

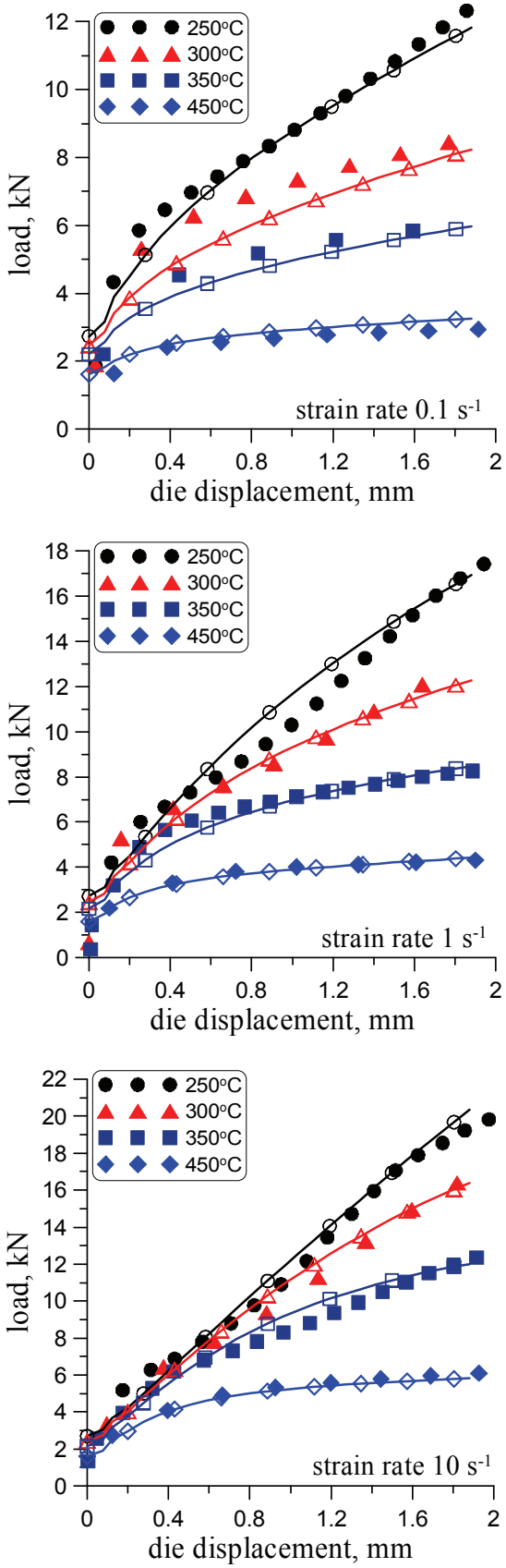

Fig. 11. Comparison of measured loads (filled symbols) with results of FE calculations using IVM model with coefficients in table 3 as rheological law (open symbols), for the AZ31 alloy. Shape of the symbol distinguishes the temperature of the test.

– Presented results confirmed qualitative predictive capability of the proposed model. Identification of the model was performed with better accuracy than for the conventional closed form equations.
– Presented approach is valid for the monotonous deformation only. The model will probably fail for processes with varying deformation path. This problem, as well as numerical solution of evolution equation (9), will be the objective of future works.

ACKNOWLEDGEMENT

Financial assistance of the MNiSzW, project no. N507 3805 33, is acknowledged.

REFERENCES

Barnett, M.R., 2003, A Taylor model based description of the proof stress of magnesium AZ31 during hot working, *Metallurgical and Materials Transactions A*, 34A, 1799-1806.

Barnett, M.R., Keshavarz, Z., Ma, X., 2006, A semianalytical Sachs model for the flow stress of a magnesium alloy, *Metallurgical and Materials Transactions A*, 37A, 2283-2293.

Beer, A.G., Barnett, M.R., 2006, Influence of initial microstructure on the hot working flow stress of Mg–3Al–1Zn, *Materials Science and Engineering A*, 423, 292–299.

Chen, C.C., Kobayashi, S., 1978, Rigid plastic finite element analysis of ring compression, application of numerical methods to forming processes, *ASME, ADM*, 28, 163-174.

Davies, C.H.J., 1994, Dynamics of the evolution of dislocation populations, *Scripta Metallurgica Materialia*, 30, 349-353.

Estrin, Y., Mecking, H., 1984, A Unified Phenomenological Description of Work Hardening and Creep Based on One-Parameter Models, *Acta Metallurgica*, 32, 57-70.

Estrin, Y., 1996, Dislocation density related constitutive modelling, *Unified constitutive laws of plastic deformation*, eds, Krausz A.S., Krausz K., Academic Press.

Forestier, R., Massoni, E., Chastel, Y., 2002, Estimation of Constitutive Parameters Using an Inverse Method Coupled to a 3D Finite Element Software, *Journal of Materials Processing Technology*, 125, 594-601.

Gavrus, A., Massoni, E., Chenot, J.-L., 1996, An Inverse Analysis using a Finite Element Model for Identification of Rheological Parameters, *Journal of Materials Processing Technology*, 60, 447-454.

Grosman, F., 1997, Problem of selection of a flow stress function for computer simulation of manufacturing, *Proc. CCME'97*, eds, Ciesielski, R., Ciszewski, B., Gronostajski, J.Z., Hawrylak, H., Kmita, J., Kobielak, S., Wrocław, I, 67-76.

Hadasik, E., Kuziak, R., Kawalla, R., Adamczyk, M., Pietrzyk, M., 2006, Rheological model for simulation of hot rolling of new generation steel strips for automotive industry, *Steel research international*, 77, 927-933.

Hansel, A., Spittel, T., 1979, *Kraft- und Arbeitsbedarf Bildsomer Formgeburgs Verfahren*, VEB Deutscher Verlag fur Grundstoffindustrie, Lipsk (in German).

Kowalski, B., Sellars, C.M., Pietrzyk, M., 2000, Development of a computer code for the interpretation of results of hot plane strain compression Tests, *ISIJ International*, 40, 1230-1236.

Lenard, J.G., Pietrzyk, M., Cser, L., 1999, *Mathematical and physical simulation of the properties of hot rolled products*, Elsevier, Amsterdam.

Madej, Ł., Pietrzyk, M., 2009, Metallic materials during processing modelled as dynamic and/or stochastic object, *Proc. Conf. CMS'09*, Kraków, 301-306.

Mecking, H., Kocks, U.F., 1981, Kinetics of flow and strain-hardening, *Acta Metallurgica*, 29, 1865-1875.

Ordon, J., Kuziak, R., Pietrzyk, M., 2000, History dependant constitutive law for austenitic steels, *Proc. Metal Forming 2000*, eds, Pietrzyk, M., Kusiak, J., Majta, J., Hartley, P., Pillinger, I., Publ. A. Balkema, Krakow, 747-753.

Prakash, A., Hochrainer, T., Reisacher, E., Riedel, H., 2008, Twinning models in self-consistent texture simulation of TWIP steels, *Steel research international*, 79, 645-652.

Pietrzyk, M., 1994, Numerical aspects of the simulation of hot metal forming using internal variable method, *Metallurgy and Foundry Engineering*, 20, 429-439.

Pietrzyk M., 2000, Finite element simulation of large plastic deformation, *Journal of Materials Processing Technology*, 106, 223-229.

Pietrzyk, M., Madej, Ł., Szeliga, D., Kuziak, R., Pidvysotskyy, V., Paul, H., Wajda, W., 2006, Rheological models of metallic materials, *Research in Polish Metallurgy at the Beginning of XXI Century*, ed., Świątkowski K., Komitet Metalurgii PAN, Kraków, 325-346.

Rauch, Ł., Madej, Ł., Węglarczyk, S., Pietrzyk, M., Kuziak, R., 2008, System for design of the manufacturing process of connecting parts for automotive industry, *Archives of Civil and Mechanical Engineering*, 8, 157-165.

Schindler, I., Hadasik, E., 2000, A new model describing the hot stress-strain curves of HSLA stell at high deformation, *Journal of Materials Processing Technology*, 106, 132-136.

Sellars, C.M., McTegart, W.J., 1966, La relation entre la resistance et la structure dans deformation a chaud, *Mem. Sci. Rev. Metall.*, 63, 731-740

Svyetlichnyy, D., 2004, *Zastosowanie technik teorii sterowania i sztucznych sieci neuronowych w modelowaniu on-line walcowania wyrobów płaskich*, Publ. Wydział Inżynierii Procesowej, Materiałowej i Fizyki Stosowanej, Politechnika Częstochowska, Częstochowa (in Polish).

Szeliga, D., Gawąd, J., Pietrzyk, M., 2006, inverse analysis for identification of rheological and friction models in metal forming, *Comp. Meth. Appl. Mech. Engrg.*, 195, 6778-6798.

Szyndler, D., Pietrzyk, M., Hodgson, P.D., 2001, Identification of parameters in the internal variable constitutive model and friction model for hot forming of steels, *Proc. NUMIFORM 2001*, ed., K. Mori, Publ. A. Balkema, Toyohashi, 297-302.

Urcola, J.J., Sellars, C.M., 1987, Effect of changing strain rate on stress-strain behaviour during high temperature deformation, *Acta Metallurgica*, 35, 2637-47.

Zienkiewicz, O.C., Taylor, R.L., 1989, *The Finite Element Method*, McGraw Hill.

FIZYCZNA I NUMERYCZNA SYMULACJA ODKSZTAŁCANIA STOPÓW MAGNEZU

Streszczenie

W artykule przedstawiono nowy model zmian struktury bazujący na zmiennych wewnętrznych i uwzględniający proces bliźniakowania. Podstawowym mechanizmem podczas odkształcania metali i stopów jest poślizg, ale w niektórych materiałach takich jak stopy magnezu lub niektóre stale, występuje również proces bliźniakowania. Zaproponowany model bazuje na metodzie zmiennej wewnętrznej, która dobrze opisuje poślizg. W modelu bliźniakowanie jest traktowane jest jako pseudo-poślizg, a zmienną zależną jest udział objętościowy bliźniaków. W pracy wykonano próby plastometryczne, a następnie przeprowadzono identyfikację modeli wykorzystując rozwiązanie odwrotne. Wyniki uzyskane dla konwencjonalnych równań algebraicznych porównano z rozwiązaniem metodą zmiennych wewnętrznych. Wykazano, że ten drugi model uwzględnia akomodację części odkształceń przez bliźniakowanie na początku procesu i, w konsekwencji, daje lepszy opis zachowania się stopu dla małych odkształceń.

Received: April 23, 2010
Received in a revised form: April 17, 2010
Accepted: May 21, 2010